

## MODELLING PHYSICAL CORRELATION OF GPS PHASE OBSERVATIONS: FIRST RESULTS

*Steffen Schön and Fritz K. Brunner*  
*Engineering Geodesy and Measurement Systems (EGMS)*  
*Graz University of Technology, Austria*  
*Email: {steffen.schoen, fritz.brunner}@tugraz.at*

**Abstract:** For precise GPS point positioning, the incomplete knowledge of the atmospheric condition along the signal path still limits the accuracy of the results. In addition, physical correlations between GPS observables are induced by the atmospheric dynamics. These correlations are usually not modelled in the variance-covariance of the observations yielding too optimistic uncertainty measures for GPS derived results.

In this contribution we present the first results of our investigations of the physical correlations of GPS signals by means of turbulence theory. The analysis is based on undifferenced observed-minus-computed values of GPS phase observations. Since the obtained time series are not always stationary, they cannot be analysed by statistical methods like autocorrelation functions. However, structure functions adequately deal with locally stationary time series. Structure functions show a power law behaviour. The power law exponent characterises the dominant stochastic process. Using temporal structure functions, the change of the power law index gives access to the decorrelation time. For the analyzed baselines we found value for the decorrelation time of 200s to 400 s depending on the amount of turbulent fluctuations encountered along the GPS signal ray paths.

### 1. Introduction

Knowledge about the effective uncertainty of GPS derived results is essential for all high precision applications. However, the commonly used stochastic models for GPS observables lead to too optimistic uncertainty measures for the results. This is mainly due to the omission of physical correlations between GPS observations which are induced by the turbulent dynamics of the atmosphere. Several investigations of the physical correlations of GPS observables are known. Three main approaches can be distinguished.

From a theoretical point of view, Schwieger [11] proposed a *forward modelling approach* to synthetically construct fully populated VCM for GPS phase observations. Following the idea of “elementary errors” proposed by [9], Schwieger identified such time dependent error sources in the a priori correction models (e.g. like the Saastamoinen [10] model) or in the auxiliary information like satellite orbits or clocks. The variance propagation of these elementary errors yields the fully populated VCM of the corrected GPS observables. He showed that the stochastic model for the tropospheric delay is decisive for the total amount of correlation. Since the satellite geometry is continuously changing, temporal as well as spatial

correlations are implicitly modelled. However, the main challenge remains in the verification of this theoretical model using actual observations.

A second approach to determine fully populated VCM – and subsequently the correlations - is based on *variance-covariance component estimation*. Tiberius and Kenselaar [12] used this approach to estimate the different covariances between code and phase observables. Computing the in-between-receiver single differences of a zero-baseline (10min, 601 epochs) they showed that: (i) the correlations between satellites of the same epoch can be neglected, (ii) correlations exist between GPS observables of the two frequencies for the analyzed Trimble 4000SSi, namely 76% between C1 and P2 and 37% between L1 and L2, while code and phase observations are uncorrelated, (iii) L1 phase observations of satellites at high elevations are free of temporal correlations, while L2 observations show temporal correlations over 10 s to 20 s. However, Tiberius and Kenselaar admitted that these zero-baseline results might not give realistic VCM for real (non-zero) baselines.

Wang et al. (2002) used also variance component estimation. They proposed an iterative stochastic assessment procedure to directly estimate the coefficients of temporal correlation of DD residuals. This strategy is based on a first order vector auto-regressive model for the DD residuals.

The third main approach attempts to derive *empirical correlation functions* fitted to the autocorrelation function of residual time series. El-Rabbany [4] found a simple exponential function with a correlation length of 263 s for L1 DD phase observations. Howind et al. [5] analysed DD residual time series (sampling rate of 15 s) of the ionospheric free linear combination for baselines from 50 km to 250 km in Antarctica. To describe the temporal correlation, they fitted four different functions to the autocorrelations functions obtained from 800 DD sequences.

However, special care must be taken to fulfil the mathematical requirements for time series analysis such as stationarity, ergodicity, homoscedaticity or normality. Bischoff et al. [2] developed statistical tests for the hypothesis of homoscedaticity.

In general, the resulting correlation functions are given in terms of exponential functions. Note that this choice of the correlation function is based on the ease of the mathematical operations and not on physical characteristics ([7], p.355).

In this paper, we present an alternative approach to treat the physical correlations of GPS signals. It is directly related to the physics of atmospheric dynamics and based on turbulence theory. Previously atmospheric turbulence theory was applied in the coordinate domain by [3]. He showed that the coordinate standard deviations of short baselines (< 3 km) follow the power law behaviour of 5/3 predicted from turbulence theory. Here, we will analyse observed-minus-computed (O-C) time series in the observation domain.

In the next section, some basic notions from turbulence theory are introduced. Then the design and the analysis of the dedicated GPS test experiment are described. First results of the application of turbulence theory for modelling physical correlation of GPS signals are presented.

## **2. Notions from turbulence theory**

*Random processes with stationary increments.* In practice, random processes are often approximated with sufficient accuracy by stationary random functions. However, due to

fluctuations these assumptions do not hold for atmospheric parameters such as temperature or refractivity. Consequently, the corresponding processes are not strictly stationary, their mean values are only constant over relatively short time periods, and the integrals describing the covariance function do not converge.

These difficulties can be overcome if these processes have stationary increments, cf. [14]. A stochastic process is said to have stationary increments if

$$\langle x(t+\Delta t) - x(t) \rangle \text{ and } \langle (x(t+\Delta t) - x(t))^2 \rangle$$

are independent of  $t$ , where the ensemble average is denoted by  $\langle \bullet \rangle$ . Therefore, the basic idea is to work with a random process

$$y(t) = x(t+\Delta t) - x(t)$$

instead of  $x(t)$ . The difference process  $y(t)$  is often stationary even if  $x(t)$  may not be stationary.

*Structure functions.* Processes with stationary increments are adequately characterised in terms of structure functions. Basically the structure function is defined for measurements  $x$  at two adjacent receivers located at the positions  $\mathbf{r}_1$  and  $\mathbf{r}_2$  and separated by the vector  $\boldsymbol{\rho}$  ([7], p. 358). The spatial structure function  $D_x(\boldsymbol{\rho})$  is defined as

$$D_x(\boldsymbol{\rho}) = \langle (x(\mathbf{r}_1) - x(\mathbf{r}_2))^2 \rangle. \quad (1)$$

It depends only on the separation  $\boldsymbol{\rho}$ . For stationary random processes, the structure and the covariance function  $B(\boldsymbol{\rho})$  are related by

$$D_x(\boldsymbol{\rho}) = 2(B(\boldsymbol{\rho}) - B(0)). \quad (2)$$

In a similar way, the temporal structure function  $D_x(\Delta t)$  is defined as

$$D_x(\Delta t) = \langle (x(t+\Delta t) - x(t))^2 \rangle = \langle (y(t))^2 \rangle. \quad (3)$$

It depends only on the temporal separation  $\Delta t$ .

*Power-law processes.* Many geophysical and atmospheric processes can be best described by so-called power-law processes, cf. [1] for an overview. For power-law processes, the spectral density  $S(f)$  is given by

$$S(f) = c f^\nu, \quad (4)$$

where  $f$  denotes the temporal or spatial frequency, and  $\nu$  the spectral index. The spectral index characterises the stochastic process, e.g. random walk processes have the index  $\nu = -2$ . For spectral indices  $\nu < -1$  the correspondent stochastic process is non-stationary. Consequently, the integral equation for the spectral density does not converge. This problem can be solved by restricting the frequency domain and eliminating mainly the low frequencies parts.

From turbulence theory we know that atmospheric fluctuations of the refractivity can be described as power law processes with an index  $\nu = -11/3$ , hence as a non-stationary process.

The corresponding structure functions for GPS phase observations shows also a power law behaviour with exponents  $5/3$  for three-dimensional turbulent processes and  $2/3$  for two-dimensional processes, respectively, cf. [7].

### 3. Experiment

#### 3.1. Set-up and Equipment

In order to study the impact of atmospheric turbulence on GPS signals, a specific test network was designed and measured by the Institute of Engineering geodesy and measurement system (EGMS).

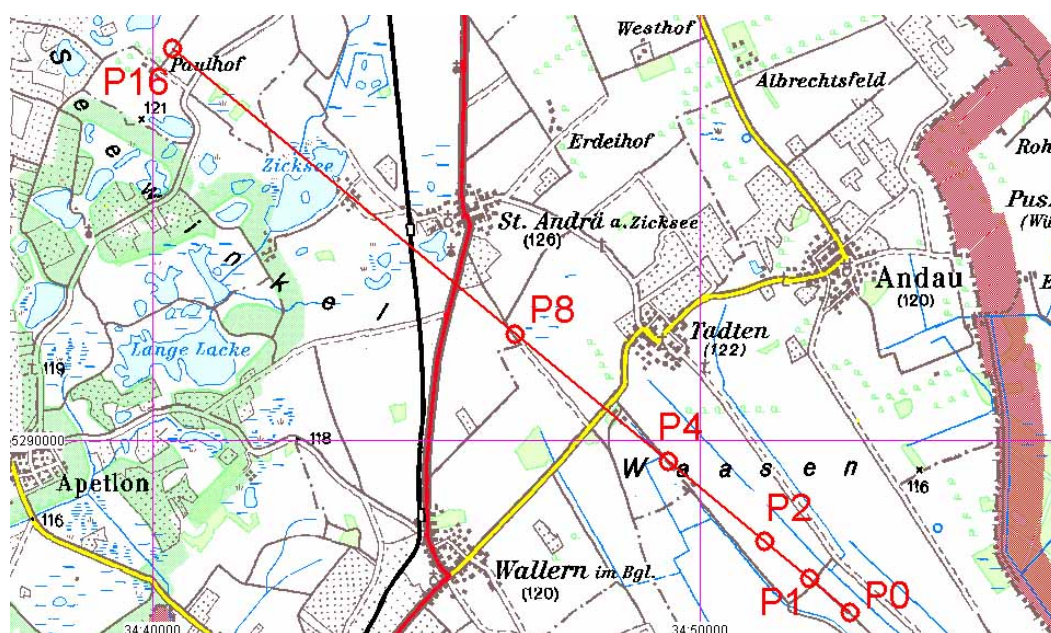


Figure 1: Test network “Seewinkel” (map by Bundesamt für Eich und Vermessungswesen)

Figure 1 shows the network design consisting of 6 points which are exactly aligned. Special care has been taken to guarantee no satellite obstructions as well as identical station heights. In addition, identical equipment was used (Leica SR530 and SR520 receiver as well as ASHTECH choke-ring antennas with SCIS-radoms) at all stations.

A 8-h session was observed using a sampling rate of 1 Hz and a cut off angle of  $3^\circ$ . In general, more than 7 satellites were tracked simultaneously. Table 1 gives an overview of the baseline lengths, height differences and azimuths.

baseline	length [km]	height difference [m]
P0-P1	0.95	0.21
P0-P2	2.04	0.19
P0-P4	4.29	1.52
P0-P8	8.00	1.70
P0-P16	16.15	-10.68

Table 1: Baseline lengths and height differences in the Seewinkel GPS network

### 3.2. Analysis

The analysis was carried out with the Bernese GPS software (vers. 5.0), cf. [6]. In a first step, the ITRF coordinates of the stations were determined with respect to the ITRF station GRAZ using 30 s data. In a second step, undifferenced L1 observed-minus-computed (O-C) time series were computed with a data rate of 1 s for the detailed analysis. For all computations, precise IGS orbits and the global CODE ionospheric model as well as precise CODE 30s satellite clocks were used. Finally, double-differences (DD) can easily be computed.

Figure 2 shows the obtained O-C DD time series using PRN6 as reference satellite for a 2h-session (5:45-7:45 GPS time, 15. April 2003) for a short baseline (P0-P1: 0.95 km) and a long baseline (P0-P16: 16.15 km). In order to improve the readability, each DD time series is shifted by a constant offset of 5 cm. Figure 3 shows the skyplot of the satellite distribution for the 2-h observation window.

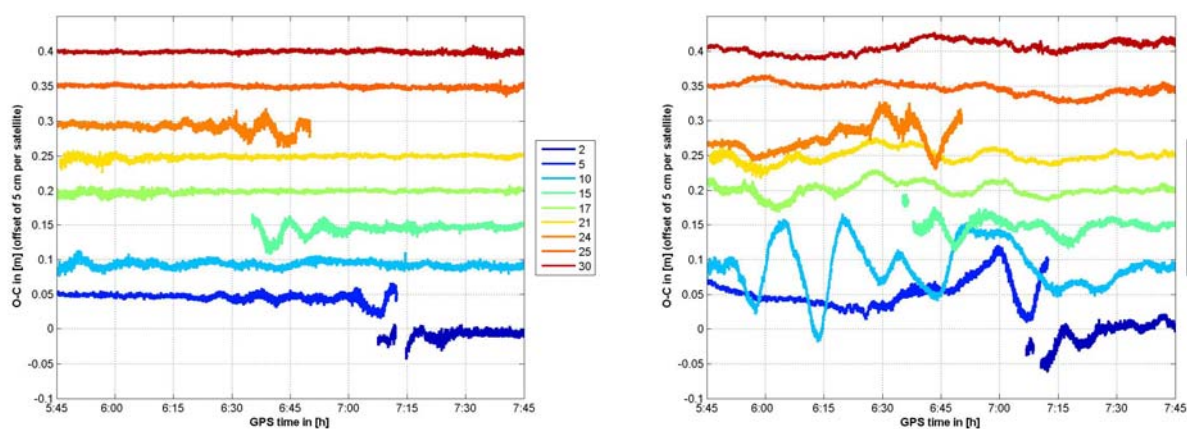


Figure 2: Time series of DD. Left: baseline P0-P1, right: baseline P0-P16

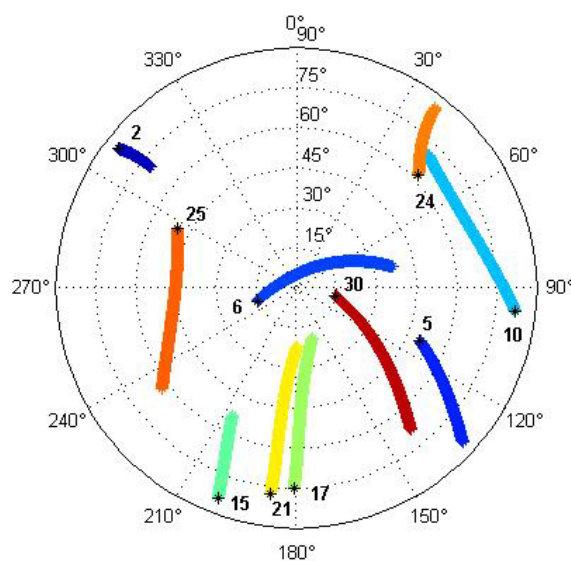


Figure 3: Skyplot of satellites during the time window (5:45-7:45)

In general, different error sources and remaining effects (after application of a priori correction models) contribute to the signatures of undifferenced GPS phase observables, such as satellite and receiver clock errors, and remaining tropospheric or ionospheric effects. Double-differencing only eliminates the common parts of the remaining effects. The residual effects in DD are reflected by trends and random variations in the time series. Their amounts increase with baseline length, compare the subfigures 2a and 2b. Since on April 15 2003 heavy ionospheric perturbation occurred ([8]), the variations (cf. Figure 2b) are mainly due to those ionospheric effects that are not modelled in the global CODE a priori correction model. These unmodelled perturbation effects can be seen from an analysis of the geometry-free linear combination – especially for PRN5, PRN10, and PRN24.

### 3.3. Temporal structure functions of DD

The temporal as well as spatial structure functions are most conveniently shown in log-log-plots, where they are straight lines with slopes equal the exponent. In section 2 the predicted exponents ( $5/3$  and  $2/3$ ) for tropospheric turbulent effects are given. In general however, different processes and error sources may be superimposed on the pure tropospheric effects in the GPS data, such as residual instrumental delays or ionospheric fluctuations. Consequently, the structure functions show several principal sections with different power law behaviours depending on the dominant effect. Figure 4 gives a typical pattern of the temporal structure function. The theoretical shape is given in red, while the pattern often encountered by actual temporal structure functions is depicted in black.

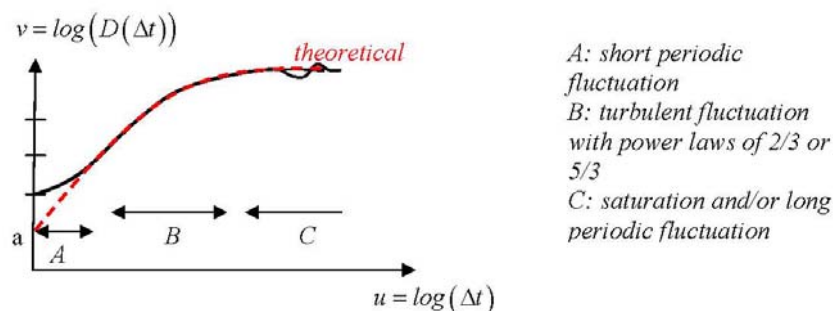


Figure 4: General behaviour of temporal structure function.

(A) For very short time differences (some seconds) the curve in the log-log-plot is flat and the corresponding power law exponent is close to 0, indicating that a white noise process is dominant.

(B) For medium time differences turbulence predominates, i.e. the steepness of the structure function in the log-log-plot increases reaching typical values of  $2/3$  and  $5/3$ .

(C) For large time differences the structure function becomes flat again with a mean power law exponent of 0. Hence, again the white noise process dominates and the data are uncorrelated. This section is called saturation. In addition, in this section, if existent, the long periodic variations of the original time series are directly reflected in the structure function.

Using precise standard products like IGS orbits, the CODE global ionospheric model, the CODE 30sec satellite clocks, and standard a priori correction models, the temporal structure

functions computed from the Seewinkel network are plotted in Figure 5. In Figure 5 these three principal sections of the structure function can be identified.

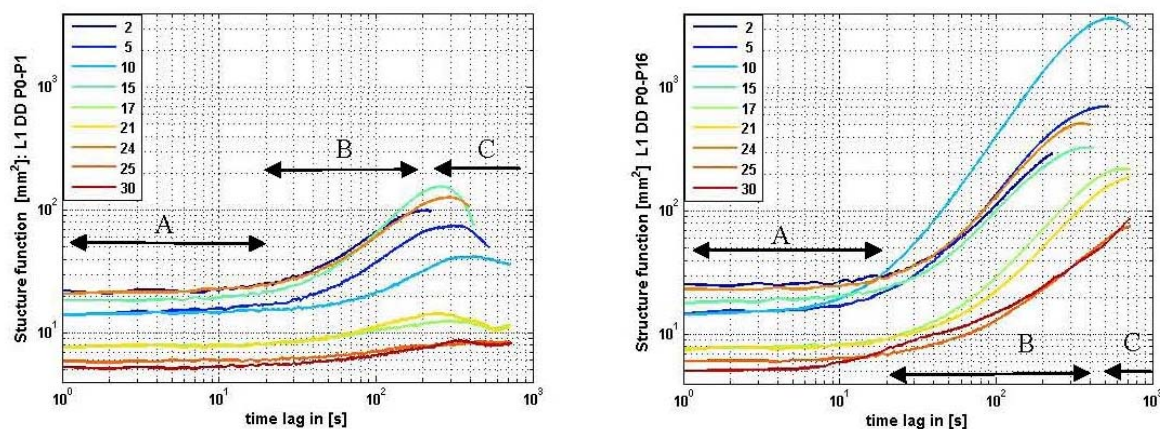


Figure 5: Temporal structure functions. Left: baseline P0-P1, right: baseline P0-P16

(A) For time lags up to 20 s the structure function is flat indicating a dominant white noise process. This process can be caused by residual instrumental effects. Using autocorrelation functions this behaviour would be reflected by a large drop of the autocorrelation in the first epoch.

(B) For larger time lags (20 s – 200 s) the steepness of the slope increases reaching maximum values between 0.2 (PRN25 and PRN30) and 1.2 (PRN15) for the short baseline. For the long baseline the power law exponent reached maximum values of 0.8 (PRN25 and PRN30) and 1.7 (PRN5 and PRN10). These values cover the predicted range and are close to  $2/3$  or  $5/3$ . Since for short baselines the remaining perturbing and turbulent effects are very similar at both endpoints, DD eliminates most of these effects which is reflected in smaller exponents. For the baseline P0-P16, in addition to tropospheric effects, ionospheric fluctuations with large temporal scales remain. From the analysis of the geometry-free linear combination, we have seen that these fluctuations show long periods of e.g., 18 min for PRN10.

(C) Finally saturation can be obtained for time lags larger than ca. 200 s or 400 s for the short baseline. This critical time lag, for which the DD are uncorrelated depends on the amount of turbulent perturbations seen by the satellites. Since for the long baselines these amounts are larger, the saturation is reached later, at time lags larger than 400 s.

#### 4. Conclusions

Using a specially design test network, we showed first results of the analysis of physical correlations treated by turbulence theory.

Structure functions have been introduced to deal in an adequate way with time series with stationary increments such as GPS DD reflecting atmospheric turbulence.

We have seen that GPS DD are composed of different stochastic processes with different power laws, such as white noise or turbulent atmospheric fluctuations.

Finally, the decorrelation time for the GPS DD depends on the amount of atmospheric fluctuations encountered along the satellites signal paths through the turbulent atmosphere. This amount is a function of the atmospheric conditions, the satellite elevations and baseline

length. Here we found decorrelation times of ca. 200 s for the 1 km baseline and larger than 400 s for the 16 km baseline.

### Acknowledgment

The first author stays as a Feodor-Lynen-Fellow with F.K. Brunner. We thank the Alexander von Humboldt-Foundation for their financial support. E. Trutmann from Rost (Vienna) and HR N. Höggerl (Bundesamt für Eich- und Vermessungswesen, Vienna) have kindly provided the Leica receivers and RTK Equipment which enabled EGMS to carry out this experiment. Their support is gratefully acknowledged by the authors. Funds for the surveying of the Seewinkel test network were provided by the Austrian Academy of Sciences for the research project "GPS Monitoring von alpinen Hangbewegungen" as part of IDNDR.

### References:

- [1] Agnew D. C.: The time-domain behaviour of power-law noises. *Geophysical research letters*, 19(4):333-336, 1992.
- [2] Bischoff W., Heck B., Howind J., Teusch A.: A procedure for testing the assumption of homoscedasticity in least squares residuals: a case study of GPS carrier-phase observations, *Journal of Geodesy*, 78:397-404, 2005.
- [3] Brunner F. K.: Zur Präzision von GPS Messungen, *Geowiss. Mitteilungen*, TU Wien, Heft 50:1-10, 1999.
- [4] El-Rabbany, A.: The Effect of Physical Correlations on the Ambiguity Resolution and Accuracy Estimation in GPS Differential Positioning. PhD dissertation. Department of Geodesy and Geomatics Engineering, Technical Report 170 University of New Brunswick. Fredericton, 1994.
- [5] Howind J., Böhringer M., Mayer M., Kutterer H., Lindner K., Heck B.: Korrelationsstudien bei GPS-Phasenbeobachtungen. In: Dietrich, R. (ed): *Deutsche Beiträge zu GPS-Kampagnen des Scientific Committee on Antarctic Research (SCAR) 1995-1998*, Deutsche Geodätische Kommission B310: 201-205, Munich, 2000.
- [6] Hugentobler U., Dach R., Fridez P. (eds): *Bernese GPS Software Version 5.0*. University of Bern, 2004.
- [7] Ishimaru, A.: *Wave Propagation and Scattering in Random Media*, Vol.2. Academic Press, New York, 1978.
- [8] NOAA: Space Environment Centre – Space Weather Alerts, <http://www.sel.noaa.gov/alerts/archive.html>
- [9] Pelzer H. (ed): *Geodätische Netze in der Landes und Ingenieurvermessung*, Wittwer, Stuttgart, 1985.
- [10] Saastamoinen, J.: Contribution to the theory of atmospheric refraction. Part II refraction corrections in satellite geodesy. *Bulletin Géodésique* 107:13-34, 1973.
- [11] Schwieger, W.: An approach to determine correlations between GPS monitored deformation epochs, In: *Proc. of the 8<sup>th</sup> International Symposium on Deformation Measurements*, Hong Kong, 17-26, 1996.
- [12] Tiberius C., Kenselaar F.: Variance Component Estimation and Precise GPS Positioning: Case study, *Journal of surveying engineering*, 129(1): 11-18, 2003.
- [13] Wang J., Satirapod C., Rizos C.: Stochastic assessment of GPS carrier phase measurements for precise static relative positioning, *Journal of Geodesy*, 76:95-104, 2002.
- [14] Yaglom, A. M.: *An introduction to the theory of stationary random functions*. Dover New York, 1962.